



# Sensor Assignment Algorithms to Improve Observability While Tracking Targets

Lifeng Zhou , *Student Member, IEEE*, and Pratap Tokekar , *Member, IEEE*

**Abstract**—In this paper, we study two sensor assignment problems for multitarget tracking with the goal of improving the observability of the underlying estimator. We consider various measures of the observability matrix as the assignment value function. We first study the general version where the sensors must form teams to track individual targets. If the value function is monotonically increasing and submodular, then a greedy algorithm yields a  $1/2$ -approximation. We then study a restricted version where exactly two sensors must be assigned to each target. We present a  $1/3$ -approximation algorithm for this problem, which holds for arbitrary value functions (not necessarily submodular or monotone). In addition to approximation algorithms, we also present various properties of observability measures. We show that the inverse of the condition number of the observability matrix is neither monotone nor submodular, but present other measures that are. Specifically, we show that the trace and rank of the symmetric observability matrix are monotone and submodular and the log determinant of the symmetric observability matrix is monotone and submodular when the matrix is nonsingular. If the target’s motion model is not known, the inverse cannot be computed exactly. Instead, we present a lower bound for distance sensors. In addition to theoretical results, we evaluate our results empirically through simulations.

**Index Terms**—Approximation assignment algorithms, nonlinear observability measures, planning, scheduling and coordination, sensor-based control.

## I. INTRODUCTION

ASSIGNING sensors to better track targets is a well-studied problem [1]–[13]. The typical setup is to formulate a one-to-one assignment problem, which can be solved using bipartite graph matching algorithms [14]. Unlike these works, we focus on scenarios where multiple sensors can be assigned to each target. Furthermore, the utility of assigning multiple sensors may not even be a simple addition of individual utilities, and can have diminishing returns. We study two versions of these many-to-one assignment problems and give constant-factor approximation algorithms for each.

Manuscript received October 21, 2018; accepted May 7, 2019. This work was supported by the National Science Foundation under Grant 1566247 and Grant 1637915. This paper was recommended for publication by Associate Editor P. Robuffo Giordano and Editor F. Chaumette upon evaluation of the reviewers’ comments. (*Corresponding author: Lifeng Zhou.*)

The authors are with the Department of Electrical and Computer Engineering, Virginia Tech, Blacksburg, VA 24060 USA (e-mail: lfzhou@vt.edu; tokekar@vt.edu).

This paper has supplementary downloadable material available at <http://ieeexplore.ieee.org>, provided by the authors. The video shows the simulation result of the paper. This material is 25.5 MB in size.

Color versions of one or more of the figures in this paper are available online at <http://ieeexplore.ieee.org>.

Digital Object Identifier 10.1109/TRO.2019.2920749

We study these assignment problems in settings where assigning the right set of sensors can improve the observability in tracking potentially mobile targets using noisy sensors. The performance of the target state estimators can be improved by exploiting the *observability* of the underlying system [15]–[18]. Our formulation is motivated by the need for reducing the load assigned to individual sensors in cooperative tracking scenarios where sensing multiple targets by the same sensor can be time-consuming or even infeasible. Following applications are reflective of such scenarios. Tokekar *et al.* [19] presented a system to track radio-tagged fish in which each radio tag is assigned a unique frequency. In order to get a measurement for one frequency, the sensor spends two seconds listening to the periodic emissions. Therefore, tracking multiple targets by the same sensor can be time-consuming. Instead, assigning each robot to a dedicated target frequency can allow for better tracking. A similar setup has been used in a number of studies on target tracking with radio sensors [20]–[22]. Such constraints are also applicable for sensors with limited fields of view [23] or with comparatively lower processing capability [24], [25], which can make it difficult to identify and/or track multiple targets for the same sensor. Motivated by these scenarios, we seek to assign sensors to track targets with the constraint that each sensor is assigned at most one target. However, multiple sensors can be assigned to track the same target. In fact, more sensors can often improve the tracking performance.

We first study a general assignment problem where there is no restriction on the number of sensors assigned to a target. We let the algorithm decide the optimal configuration of sensor teams assigned to each target. If the value function is submodular and monotone,<sup>1</sup> a greedy algorithm gives a  $1/2$ -approximation [26]. In general, this bound is tighter, i.e.,  $1 - 1/e$  by using the randomized continuous greedy algorithm [27]. However, for a deterministic algorithm,  $1/2$ -approximation is the best-known result [27]. We show that observability measures such as the trace and rank of the symmetric observability matrix are submodular and monotone and the log determinant is submodular and monotone when the symmetric observability matrix is nonsingular. However, the inverse of the condition number, a commonly used measure, is neither monotone nor submodular, which we show by a counterexample.

We then study a *restricted* version of the problem where the value function can be arbitrary (not necessarily monotone and submodular) but exactly two sensors must be assigned to a target. In fact, we show in Corollaries 1 and 2 that at least two

<sup>1</sup>We use “monotone” and “monotone increasing” interchangeably.

range sensors must be assigned for the inverse condition number to be greater than zero. Even for the case of bearing sensors, it is known that two sensors are necessary; there exists work on assignment and placement of pairs of bearing sensors for improving target tracking [5], [7]. We study the analogous problem for range sensors. We prove that the greedy algorithm achieves a 1/3-approximation of the optimal solution for assigning pairs of range sensors.

Observability is a basic concept in control theory and has been widely applied in robotics. Observability for range-only beacon sensors, in particular, has been closely studied for underwater navigation. Gadre and Stilwell [15] analyzed the local and global observability [28] for the localization of an autonomous underwater vehicle by an acoustic beacon. The problems of single vehicle localization and multivehicle relative localization are studied in [17] using an observability criterion introduced in [29]. In these works, it is the sensors that are moving. Consequently, the sensors know their control vectors and can thus compute the observability matrix and its measures. When tracking a target, however, the control inputs for the targets may be unknown. In recent work, Williams and Sukhatme [18] studied a multisensor localization and target tracking problem where they showed how to leverage graph rigidity to improve the observability for sensor team localization and robust target tracking.

Unlike these works, we consider scenarios where the control inputs for the targets are not known to the sensors. Consequently, we cannot compute the observability matrix exactly. Instead, we present a novel lower bound on the observability for the case of unknown target motion tracked by range-only sensors. Specifically, we show how to lower bound the *condition number* [29] of the partially known observability matrix using only the known part (see Section III). The result is specific to the problem at hand where the inputs appear, linearly, on a single line of the observability matrix.

In addition to theoretical results, we conduct simulations to evaluate the empirical performance of the algorithms. We find that sensors are assigned to targets almost uniformly using the greedy algorithm for the first problem (see Section V-A). The greedy algorithm for the second problem performs much better than 1/3 in practice (see Section V-B).

## II. OVERVIEW OF THE PROBLEM AND RESULTS

In this section, we first formally define the problems that are studied and then summarize the main contributions of this paper.

### A. Problem Formulation

We consider a scenario where there are  $N$  sensors and  $L$  targets in the environment. We use  $\sigma(t_l)$  to represent the set of sensors assigned to target  $t_l$ .  $\sigma^{-1}(s_i)$  gives the set of targets assigned to sensor  $s_i$ . We use  $\sigma_i(t_l)$  to give the  $i$ th sensor assigned to target  $t_l$ . We order the assigned sensors by using their IDs such that  $\sigma_1(t_l) < \sigma_2(t_l) < \sigma_3(t_l) < \dots$ . Let  $\omega(s_i, s_j, t_l)$  and  $\omega(\mathcal{S}_i, t_l)$  be some measure of the observability of tracking  $t_l$  with  $s_i$  and  $s_j$ , and with a set of sensors  $\mathcal{S}_i$ , respectively. We

calculate the observability measure by taking account of the relative positions of sensors and targets (which will appear in the observability matrix) at every time step.

We start with the problem of assigning a set of sensors to each target. The sensors form teams of varying sizes to track individual targets. Sensors within a team can share measurements so as to better track the targets. We constrain each sensor to be assigned to only one target. This is motivated by scenarios where sensing multiple targets can be time-consuming (as is the case with radio sensors [19], [30]) or communicating multiple measurements with the team can be energy and time-consuming.

*Problem 1 (General Assignment):* Given a set of sensors,  $\mathcal{S} := \{s_0, \dots, s_N\}$ , and a set of targets,  $\mathcal{T} := \{t_0, \dots, t_L\}$ , find an assignment of sets of sensors targets to

$$\text{maximize } \sum_{l=1}^L \omega(\sigma(t_l), t_l) \quad (1)$$

with the added constraint that each sensor is assigned to at most one target.

Problem 1 is the general assignment problem, which is difficult to solve for arbitrary  $\omega(\cdot)$ . In order to solve the assignment problem for arbitrary value functions, we consider a restricted case where each target is tracked by exactly two sensors.

*Problem 2 (Nonoverlapping Pair Assignment):* Given a set of sensors,  $\mathcal{S} := \{s_0, \dots, s_N\}$ , and a set of targets,  $\mathcal{T} := \{t_0, \dots, t_L\}$ , find an assignment of nonoverlapping pairs of sensors targets to

$$\text{maximize } \sum_{l=1}^L \omega(\sigma_1(t_l), \sigma_2(t_l), t_l) \quad (2)$$

with the added constraint each sensor is assigned to at most one target. That is, for all  $i = 1, \dots, N$  we have  $|\sigma^{-1}(s_i)| \leq 1$ , assuming  $N \geq 2L$ .

In fact, we show in Corollaries 1 and 2 that at least two sensors are necessary for certain observability measure of range sensors. Even for the case of bearing sensors, it is known that two sensors are necessary; there exists work on assignment and placement of pairs of bearing sensors for improving target tracking [5], [7].

### B. Contributions

The main contributions of this paper are summarized as follows.

- 1) We derive a lower bound on the inverse of the condition number of the observability matrix, which is useful when the control input for the target is not known.
- 2) We show that the condition number of the observability matrix is neither submodular nor monotone increasing. We show that the trace and the rank of the symmetric observability matrix are submodular and monotone increasing. We also show the log determinant of the symmetric observability matrix is submodular and monotone when the symmetric observability matrix is nonsingular.
- 3) We present a greedy assignment algorithm that yields a 1/2-approximation for Problem 1 and 1/3-approximation for Problem 2.

- 4) We verify the performance of our proposed greedy algorithm with various observability measures (that not necessary submodular) through extensive simulations.

We start by showing how to bound the inverse of condition number (see Section III) and then present the assignment algorithms (see Section IV).

### III. BOUNDING THE OBSERVABILITY

Consider a mobile target  $t_l$  whose position is denoted by  $p_{t_l}$ . Suppose there are  $N$  stationary sensors that can measure the distance<sup>2</sup> to the target. We have

$$\begin{cases} \dot{p}_{t_l} = u_{t_l} \\ z_{s_i} = h_i(p_{t_l}) = \frac{1}{2} \|p_{s_i} - p_{t_l}\|_2^2 + v_{s_i}, \quad i = 1, \dots, N \end{cases} \quad (3)$$

where  $p_{t_l} := [x_{t_l}, y_{t_l}]^T$  gives the two-dimensional (2-D) position of the target, and  $u_{t_l} := [u_{lx}, u_{ly}]$  defines its control input, which is unknown to the sensor. Let  $u_{t_l, \max} \triangleq \max \|u_{t_l}\|_2$  and let  $z_{s_i}$  denote the range-only measurement from each sensor  $s_i$  whose position is given by  $p_{s_i} = [x_{s_i}, y_{s_i}]^T$ . Further, let  $v_{s_i}$  denote the zero mean Gaussian noise of sensor  $s_i$ , which is independent of the states  $p_{s_i}$  and  $p_{t_l}$ . The state-independent noise model is used in many observability-based studies [16]–[18], [31], [32]. For simplicity, we also assume that the target does not collide with any sensor, i.e.,  $\|p_{s_i} - p_{t_l}\|_2 \neq 0$  and no two sensors are deployed at the same position.

We analyze the weak local observability matrix,  $O(p_{t_l}, u_{t_l})$ , of this multisensor-target tracking system. We show how to lower bound the inverse of the condition number of  $O(p_{t_l}, u_{t_l})$ , given by  $C^{-1}(O(p_{t_l}, u_{t_l}))$ , independent of  $u_{t_l}$ . We also show that the lower bound,  $\underline{C}^{-1}(O(p_{t_l}, u_{t_l}))$ , is tight.

We compute the local nonlinear observability matrix by using Lie derivatives [18], [28] for this system [see (3)] as

$$O(p_{t_l}, u_{t_l}) = \begin{bmatrix} \nabla L_0^{h_1} \\ \nabla L_1^{h_1} \\ \vdots \\ \nabla L_0^{h_2} \\ \nabla L_1^{h_2} \\ \vdots \\ \vdots \\ \nabla L_0^{h_N} \\ \nabla L_1^{h_N} \\ \vdots \end{bmatrix} = \begin{bmatrix} x_{t_l} - x_{s_1}, y_{t_l} - y_{s_1} \\ u_{lx}, u_{ly} \\ 0, 0 \\ \vdots \\ x_{t_l} - x_{s_2}, y_{t_l} - y_{s_2} \\ u_{lx}, u_{ly} \\ 0, 0 \\ \vdots \\ \vdots \\ x_{t_l} - x_{s_N}, y_{t_l} - y_{s_N} \\ u_{lx}, u_{ly} \\ 0, 0 \\ \vdots \end{bmatrix}. \quad (4)$$

This equation can be rewritten as

$$O(p_{t_l}, u_{t_l}) = \begin{bmatrix} x_{t_l} - x_{s_1}, y_{t_l} - y_{s_1} \\ x_{t_l} - x_{s_2}, y_{t_l} - y_{s_2} \\ \vdots \\ x_{t_l} - x_{s_N}, y_{t_l} - y_{s_N} \\ u_{lx}, u_{ly} \end{bmatrix}_{(N+1) \times 2}. \quad (5)$$

The state of the target  $t_l$  is *weakly locally observable* if the local nonlinear observability matrix has full column rank [28]. However, the rank test for the observability of the system does not tell the degree of the observability or how *good* the observability is. The *condition number* [29], defined as the ratio of the largest singular value to the smallest, can be used to measure this degree of unobservability. We use the *inverse of condition number* given as

$$C^{-1}(O(p_{t_l}, u_{t_l})) = \frac{\sigma_{\min}(O(p_{t_l}, u_{t_l}))}{\sigma_{\max}(O(p_{t_l}, u_{t_l}))}. \quad (6)$$

Note that  $C^{-1} \in [0, 1]$ .  $C^{-1} = 0$  means  $O(p_{t_l}, u_{t_l})$  is singular and  $C^{-1} = 1$  means  $O(p_{t_l}, u_{t_l})$  is *well-conditioned*. A larger  $C^{-1}$  means better observability (see more details in [17]).

In the local nonlinear observability matrix  $O(p_{t_l}, u_{t_l})$ ,  $u_{t_l}$  is unknown and not controllable by the sensor. On the other hand,  $p_{t_l} - p_{s_i}$  depends on the relative state between each sensor  $s_i$  and target  $t_l$  and is known to the sensor (assuming an estimate of the target's position is known). Thus, we first partition  $O(p_{t_l}, u_{t_l})$  into the known and unknown parts as

$$O(p_{t_l}, u_{t_l}) = \begin{bmatrix} O(p_{t_l}) \\ O(u_{t_l}) \end{bmatrix} \quad (7)$$

where

$$O(p_{t_l}) := \begin{bmatrix} x_{t_l} - x_{s_1}, y_{t_l} - y_{s_1} \\ x_{t_l} - x_{s_2}, y_{t_l} - y_{s_2} \\ \vdots \\ x_{t_l} - x_{s_N}, y_{t_l} - y_{s_N} \end{bmatrix} \quad (8)$$

and

$$O(u_{t_l}) := [u_{lx}, u_{ly}] \quad (9)$$

indicate the contributions from the sensor-target relative state and target's control input, respectively. Since  $O(u_{t_l})$  is unknown, we cannot compute  $C^{-1}(O(p_{t_l}, u_{t_l}))$  exactly. Instead, we compute its lower bound as shown in the following.

*Theorem 1:* For the multisensor-target system [see (3)] with the number of sensors,  $N \geq 2$ , the inverse of the condition number is lower bounded by

$$\frac{\sigma_{\min}(O(p_{t_l}))}{\sqrt{\sigma_{\max}^2(O(p_{t_l})) + u_{t_l, \max}^2}}.$$

We present the full proof for this and other results in the appendix.

We wish to improve the worst case, i.e., the lower bound of  $C^{-1}(O(p_{t_l}, u_{t_l}))$ , by optimizing the sensor-target relative state

<sup>2</sup>We use the square of the distance/range for mathematical convenience.

by assigning a different subset of sensors to the target. In the following, we will show that at least two sensors are required to improve the lower bound.

*Corollary 1:* The lower bound of the observability metric in one-sensor-target system,  $\underline{C}^{-1}(O_i(p_{t_l}, u_{t_l}))$ , is identically zero. It does not depend on the position of the sensor and therefore cannot be controlled by the sensors.

When the number of sensors  $N \geq 2$ , we have a positive result that shows that the sensors can improve the lower bound on the inverse of the condition number of optimizing their positions, even though the contribution to the observability matrix from the target's input,  $O(u_{t_l})$ , is unknown and cannot be controlled.

*Corollary 2:* Suppose that the number of sensors assigned to  $t_l$ ,  $N \geq 2$ . If the sensors increase  $C^{-1}(O(p_{t_l}))$  and  $\sigma_{\min}(O(p_{t_l}))$  [the inverse of condition number and the smallest singular number of the relative state contribution  $O(p_{t_l})$ ], then the lower bound of  $C^{-1}(O(p_{t_l}, u_{t_l}))$  also increases.

*Remark 1:* The lower bound  $\underline{C}^{-1}(O(p_{t_l}, u_{t_l}))$  is tight when the target is known to be stationary. If  $u_o \in \{0\}$ ,  $O(p_{t_l}, u_{t_l}) = O(p_{t_l})$  by (5) and (8). Thus, from (6) and Theorem 1, the lower bound  $\underline{C}^{-1}(O(p_{t_l}, u_{t_l})) = C^{-1}(O(p_{t_l}, u_{t_l}))$ , which implies that the lower bound is tight.

Next, we use these results for assigning sensors to targets.

#### IV. ASSIGNMENT ALGORITHMS

So far, we have assumed that we know the true position,  $p_{t_l}(k)$ , of the target at time  $k$ . In practice, we only have an estimate,  $\hat{p}_{t_l}(k)$ , for  $t_l$  along with its covariance  $\Sigma_{t_l}(k)$ . The estimate is obtained by fusing measurements using, for example, an extended Kalman filter (EKF). We use the estimated position of the target for the assignment algorithms in the simulation (see Section V). This is a cyclical problem—in order to compute the assignment to better estimate the state, we need an estimate of the state to begin with. In practice, an initial estimate is present based on some domain-specific information [33].

##### A. General Assignment as Submodular Welfare Optimization

We first study the general assignment (Problem 1) where each target  $t_l$  is tracked by a subset of sensors  $\sigma(t_l) \subset \mathcal{S}$ ,  $l \in \{1, 2, \dots, L\}$  whose cardinality is not necessarily two. This is known as *submodular welfare problem* in the literature [27] where the objective is to maximize  $\sum_{i=1}^n w_i(\mathcal{S}_i)$  for independent sets  $\{\mathcal{S}_i | \mathcal{S}_i \subseteq \mathcal{S}, i = \{1, 2, \dots, n\}\}$  by using monotone and submodular utility functions  $w_i$ . A greedy algorithm [26] yields a  $1/2$ -approximation for this problem. We first show that the lower bound of the inverse of the condition number is neither monotone nor submodular. This is not surprising since it has been shown that similar measures for analogous versions of the controllability matrix are also not submodular or monotone increasing [34].

*Theorem 2:* The lower bound of the inverse of condition number function  $\omega(\cdot)$  is neither monotone increasing nor submodular.

*Proof:* We prove the claim by giving two counterexamples.

*Case 1:* Given the sensors  $s_1(0, 0)$ ,  $s_2(2\sqrt{3}, -9)$ ,  $s_3(\sqrt{3}, 3)$  and target  $t_1(\sqrt{3}, 1)$  with  $u_{t_1, \max} = 1$  in 2-D plane,

---

##### Algorithm 1: Greedy Non-overlapping Pair Assignment.

---

```

 $k \leftarrow 0$ ,  $\omega(\text{GREEDY}) \leftarrow 0$ 
while true do
  Compute all possible  $\omega(\sigma_1(t_l), \sigma_2(t_l), t_l)$ .
  Pick the triple  $(\sigma_1(t_l), \sigma_2(t_l), t_l)$  with maximum
   $\omega(\sigma_1(t_l), \sigma_2(t_l), t_l)$  defined as  $\omega_{\max}$ .
   $\omega(\text{GREEDY}) \leftarrow \omega(\text{GREEDY}) + \omega_{\max}$ .
  Remove  $\{s_i, s_j\}$  from the sensor set  $\mathcal{S}$  and remove  $t_l$ 
  from the target set  $\mathcal{T}$ .
   $k \leftarrow k + 1$ 
end

```

---

$\omega(\{s_1, s_3\}) = 0.5345 > \omega(\{s_1, s_2, s_3\}) = 0.1823$ , which shows  $\omega(\cdot)$  is not monotone increasing.

*Case 2:* Given the sensors  $s_1(0, 0)$ ,  $s_2(2\sqrt{3}, 0)$ ,  $s_3(\sqrt{3}, 0.1)$ ,  $s_4(\sqrt{3}, 3)$  and target  $t_1(\sqrt{3}, 1)$  with  $u_{t_1, \max} = 1$  in 2-D plane,  $\omega(\{s_1, s_2, s_3\}) - \omega(\{s_1, s_2\}) = 0.3310 - 0.5345 = -0.2035 < \omega(\{s_1, s_2, s_4, s_3\}) - \omega(\{s_1, s_2, s_4\}) = 0.8765 - 0.9258 = -0.0493$ , which shows  $\omega(\cdot)$  is not submodular. ■

Therefore, we focus on other measures of observability and summarize the results in Corollary 3.

*Corollary 3:* A corollary of [34, Ths. 4, 6, and 7]. The trace and rank of the symmetric observability matrix,  $\mathbb{O}(p_{t_l}, u_{t_l}) := O^T(p_{t_l}, u_{t_l})O(p_{t_l}, u_{t_l})$ , and of the sensor-target relative state contribution matrix,  $\mathbb{O}(p_{t_l}) := O^T(p_{t_l})O(p_{t_l})$ , are submodular/modular and monotone increasing. The log determinant of the two matrices is submodular and monotone increasing if the corresponding matrix is nonsingular.

The reason that we also study the measures of the symmetric observability matrix by sensor-target relative state contribution is that the control input of the target is unknown, and thus the symmetric observability matrix is not available. The proof provided in the appendix is similar to proving that the trace of the Gramian is modular, and the log determinant, and the rank of the Gramian are monotone submodular [34]. Note that if  $\mathbb{O}(p_{t_l})$  is singular, its log determinant is  $-\infty$ . In our sensor assignment case, if a single sensor is assigned to target  $t_l$ ,  $\mathbb{O}(p_{t_l})$  is always singular, i.e.,  $\det(\mathbb{O}(p_{t_l})) = 0$  (see the proof of Corollary 1). If no sensors are assigned to a target, then the matrix is not defined. Thus, at least two sensors need to be assigned to a target to ensure nonsingularity of  $\mathbb{O}(p_{t_l})$ .

##### B. 1/3-Approximation Algorithm for Problem 2

Next, we study a more specific assignment (Problem 2) where each target  $t_l$  is tracked by a pair of sensors but allow the value function to be arbitrary. We propose a greedy algorithm to solve this problem. In each round, we calculate the observability metric  $\omega(\sigma_1(t_l), \sigma_2(t_l), t_l)$  for all triples  $(\sigma_1(t_l), \sigma_2(t_l), t_l)$ ,  $\sigma_1(t_l), \sigma_2(t_l) \in \mathcal{S}$ ,  $t_l \in \mathcal{T}$ , and select the triple that has the maximum  $\omega(\sigma_1(t_l), \sigma_2(t_l), t_l)$ , then remove  $\{\sigma_1(t_l), \sigma_2(t_l)\}$  from sensor set  $\mathcal{S}$  and remove  $t_l$  from target set  $\mathcal{T}$ , respectively. We present the greedy approach in Algorithm 1 where  $\omega(\text{GREEDY})$  denotes total value obtained by the greedy approach. In this case, we can use the inverse of the condition number as  $\omega(\cdot)$ .

*Theorem 3:*  $\omega(\text{GREEDY}) \geq \frac{1}{3}\omega(\text{OPT})$  where OPT is the optimal algorithm for Problem 2. The running time for Algorithm 1 is  $O(N^2L^2)$ .

*Proof:* We first give the proof for the approximation ratio of Algorithm 1. Recall that  $\omega(\text{GREEDY})$  and  $\omega(\text{OPT})$  will be the sum of  $\omega(\cdot)$  terms of triples consisting of one target and the two assigned sensors. As a shorthand, we will denote  $\omega^g(l)$  and  $\omega^*(l)$  to be the values of the triple assigned to  $t_l$  by GREEDY and OPT, respectively.

We show that there exists a many-to-one mapping  $\mathcal{M} : [1, \dots, L] \rightarrow [1, \dots, L]$  such that the following conditions hold:

- 1)  $\omega^*(k) \leq \omega^g(\mathcal{M}(k))$ ;
- 2)  $|\mathcal{M}^{-1}(y)| \leq 3$  for all  $y \in \mathcal{Y}$ , where  $\mathcal{Y} \subseteq [1, \dots, L]$  is the range of  $\mathcal{M}$ .

That is, each triple in OPT is mapped to some triple in GREEDY whose value is at least as high and no triple in GREEDY has more than three terms in OPT mapped to it.

We first show that if such a mapping exists, then the main result holds. Then, we prove the existence of such a mapping by constructing a specific  $\mathcal{M}$ .

If such a mapping  $\mathcal{M}$  exists, we prove  $\omega(\text{GREEDY}) \geq \frac{1}{3}\omega(\text{OPT})$  as follows:

$$\begin{aligned}
 \omega(\text{OPT}) &= \sum_{k=1}^L \omega^*(k) \leq \sum_{k=1}^L \omega^g(\mathcal{M}(k)) \\
 &= \sum_{y \in \mathcal{Y}} \omega^g(y) |\mathcal{M}^{-1}(y)| \\
 &\leq 3 \sum_{y \in \mathcal{Y}} \omega^g(y) \leq 3 \sum_{l=1}^L \omega^g(l) \\
 &= 3\omega(\text{GREEDY}). \tag{10}
 \end{aligned}$$

The first inequality is due to  $\omega^*(k) \leq \omega^g(\mathcal{M}(k))$ . The second equality is because  $\mathcal{M}$  maps each item in  $[1, \dots, L]$  to the set  $\mathcal{Y}$ . The second inequality is due to  $|\mathcal{M}^{-1}(\cdot)| \leq 3$ . The third inequality is because  $\mathcal{Y} \subseteq [1, \dots, L]$ .

Next, we show that such a mapping always exists by constructing one. We will define  $\mathcal{M}$  in the order in which the triples are picked by GREEDY. Suppose GREEDY picks the triple  $(s_i, s_j, t_l)$  in some round. Then,  $\omega^g(l) = \omega(s_i, s_j, t_l)$ . We will map at most three triples in OPT to this triple in GREEDY. There are following three cases.

- 1)  $(s_i, s_j, t_l)$  is also chosen by OPT [see Fig. 1(a)]. If  $\mathcal{M}(l)$  has not been defined in previous rounds, we define  $\mathcal{M}(l) = l$ . Note that here  $\omega^g(l) = \omega^*(l)$  and  $|\mathcal{M}^{-1}(l)| = 1$ . Therefore, the two conditions for a valid mapping are satisfied.
- 2) Exactly two of  $(s_i, s_j, t_l)$  appear in a triple chosen by OPT [see Fig. 1(b)]. Consider the case where OPT chooses  $(s_i, s_j, t_m)$  and  $(s_p, s_q, t_l)$  where  $m \neq l$ . All other cases are symmetric. If  $\mathcal{M}(m)$  has not been defined in a previous round, we define  $\mathcal{M}(m) = l$ . Note that if  $\mathcal{M}(m)$  was not defined in a previous round, then  $\omega^*(m) \leq \omega^g(l)$ . Otherwise, GREEDY would pick the triple  $(s_i, s_j, s_m)$  in

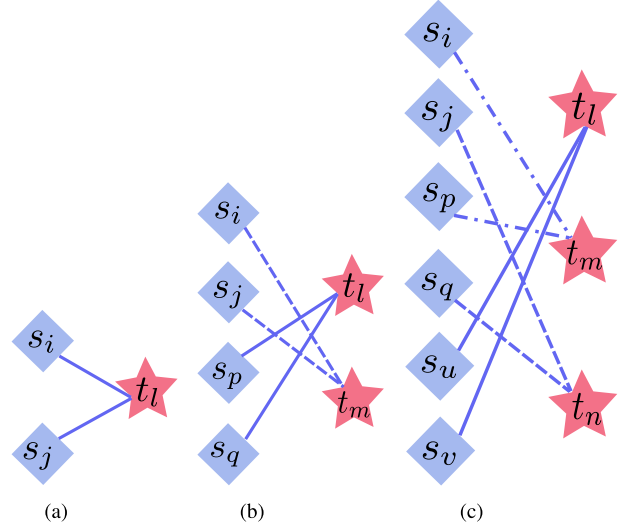


Fig. 1. Optimal solution in three cases. In all cases, the GREEDY chooses the triple  $(s_i, s_j, t_l)$ . (a) Case 1: The OPT charges  $\omega(s_i, s_j, t_l)$  to the same triple  $(s_i, s_j, t_l)$  chosen by the GREEDY. (b) Case 2: The OPT charges  $\omega(s_i, s_j, t_l)$  to at most two triples— $(s_i, s_j, t_m)$  and  $(s_p, s_q, t_l)$ . (c) Case 3: The OPT charges  $\omega(s_i, s_j, t_l)$  to at most three triples— $(s_i, s_p, t_m)$ ,  $(s_j, s_q, t_n)$ , and  $(s_u, s_v, t_l)$ . Here,  $i \neq j \neq p \neq q \neq u \neq v$  and  $l \neq m \neq n$ .

this round. Similarly, if  $\mathcal{M}(l)$  is not defined in a previous round, we define  $\mathcal{M}(l) = l$ . By a similar argument, if  $\mathcal{M}(l)$  was not defined in a previous round,  $\omega^*(l) \leq \omega^g(l)$ . Furthermore,  $|\mathcal{M}^{-1}(l)| = 2$ . Therefore, the two conditions for a valid mapping are satisfied.

- 3) No two of  $(s_i, s_j, t_l)$  appear in the same triple chosen by OPT. Suppose instead they appear in three distinct triples,  $(s_u, s_v, t_l)$ ,  $(s_i, s_p, t_m)$ , and  $(s_j, s_q, t_n)$ , as shown in Fig. 1(c). We can use a similar argument as in the previous case. If any of  $l, m$ , and  $n$  were not mapped in a previous round, then we will map them to  $l$ . Furthermore, since they were not mapped in a previous round, their value in OPT cannot be greater than  $\omega^g(l)$ . Finally,  $|\mathcal{M}^{-1}(l)| \leq 3$ . Therefore, the two conditions for a valid mapping are satisfied.

Therefore, given such a mapping  $\mathcal{M}$ , it follows that  $\omega(\text{GREEDY}) \geq \frac{1}{3}\omega(\text{OPT})$ .

We next prove the running time for Algorithm 1. The “while” loop runs for  $L$  rounds since all the targets must be tracked eventually. Inside the “while” loop, we compute all possible triples and find the best one. This requires  $O(N^2L)$  time. Overall, Algorithm 1 runs in  $O(N^2L^2)$  time. ■

*Remark 2:* It is possible to generalize this result to the case where exactly  $n$  sensors are to be assigned to a target with  $n \geq 2$ . We can obtain a generalized bound,  $\omega(\text{GREEDY}) \geq \frac{1}{n+1}\omega(\text{OPT})$ , by using a proof similar to that of Theorem 3.

A proof sketch is given in the appendix.

## V. SIMULATIONS

We illustrate the performance of the assignment strategies for sensor selection using observability measure as the performance

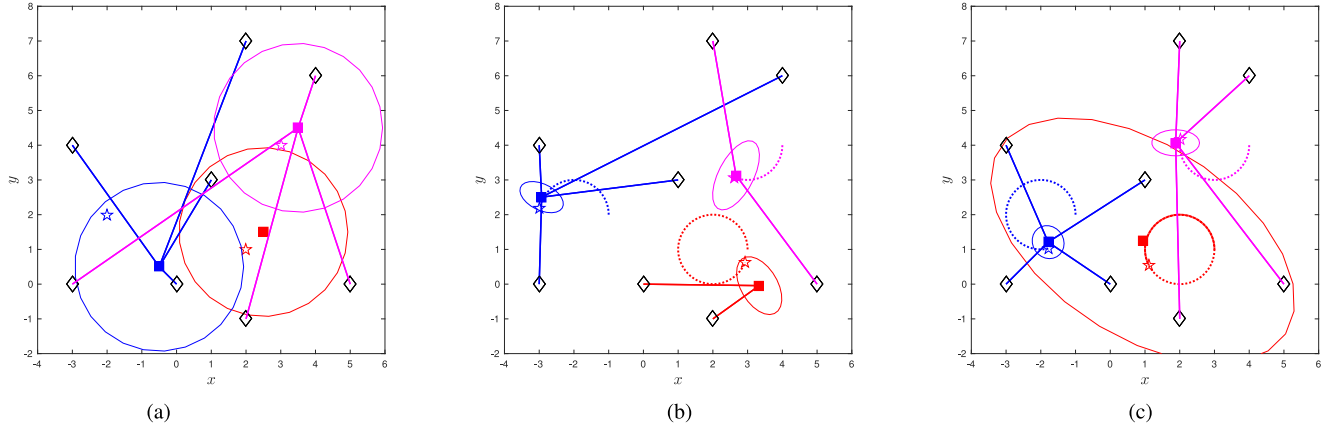


Fig. 2. Greedy general assignment [26] in action for tracking three targets with a circular motion by using  $\text{trace}(\mathbb{O}(p_{t_l}))$ . The three colors red, blue, and magenta specify three targets, respectively. The pentagram, filled square, solid ellipse (sometimes, it looks like a solid circle), and the dotted circle indicate the true position, estimate mean position, variance, and trajectory for the target, respectively. The black diamond indicates the sensor. The solid line joining the target and sensor indicates that the sensor is assigned to the target. (a)  $k = 1$  (initial time). (b)  $k = 60$ . (c)  $k = 100$ .

criterion. A video showing the algorithm in action is submitted as supplementary material.

#### A. Greedy General Assignment

We first simulate the greedy assignment [26] for Problem 1 by using the trace of the *symmetric observability matrix by sensor-target relative state contribution*,  $\text{trace}(\mathbb{O}(p_{t_l}))$  as observability measure that is monotone and submodular/modular as shown in Corollary 3. Notably, for maximizing a modular function, the greedy algorithm yields an optimal solution. We start with the greedy assignment with eight stationary sensors and three targets moving in a circle and  $u_{t_l, \max} = 1$ ,  $l \in \{1, 2, 3\}$  within 100 time steps in a  $10 \times 10$  environment. At each time step, we use the greedy approach [26] to assign a set of sensors to each target, and use the measurements of the set of sensors to update the estimate of the target by EKF, as shown in Fig. 2. Notably, some targets [say the red target in Fig. 2(a) and (c)] are left untracked. This is because, in the general assignment (Problem 1), the size of the set of sensors assigned to each target is flexible. The objective of the assignment is to maximize the summation of the observability measures from all the targets [see (1)] instead of maximizing the worst case observability measure (say the red target). Thus, in order to maximize the summation, some target can be sacrificed, that is, left untracked. One idea for improving the tracking performance is to assign at least two sensors to each target. However, for this constraint, it is challenging to come up with a polynomial-time optimal algorithm or approximation algorithm. We can find a feasible assignment in polynomial time by first assigning a pair of sensors to each target by Algorithm 1 and then perform the greedy general assignment for the following sensors. However, the performance of the combination of these two greedy algorithms cannot be readily bounded and is an avenue of future work.

In order to further evaluate the greedy approach for the general assignment, we set the number of targets as  $L = 5$  and number of sensors,  $N$ , from 20 to 50. For each  $N \in \{20, 21, \dots, 50\}$ , the

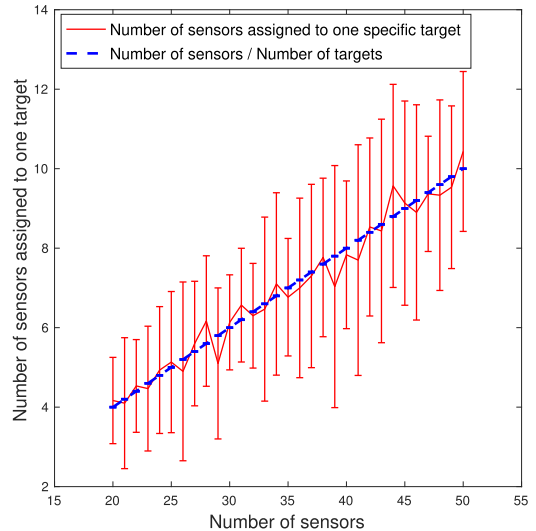


Fig. 3. Number of sensors assigned to each target.

positions of sensors and targets are randomly generated within  $[0, 100] \times [0, 100] \in \mathbb{R}^2$  for 30 trials. We compare the number of sensors assigned to one specific target, i.e.,  $t_l, l \in \{1, 2, \dots, L\}$  with the  $N/L$ , as shown in Fig. 3. It shows that the sensors are assigned to each target almost evenly.

#### B. Greedy Nonoverlapping Pair Assignment

We then simulate the greedy nonoverlapping pair assignment (Algorithm 1) for solving Problem 2. With the same environment setting, we start with simulating Algorithm 1 with  $\text{trace}(\mathbb{O}(p_{t_l}))$  as the observability measure (see Fig. 4). We know that the observability measure for greedy nonoverlapping pair assignment does not have to be monotone submodular. Therefore, we use the log determinant of the *symmetric observability matrix by sensor-target relative state contribution*,  $\log \det(\mathbb{O}(p_{t_l}))$ , and the lower bound on the inverse of the condition number of the

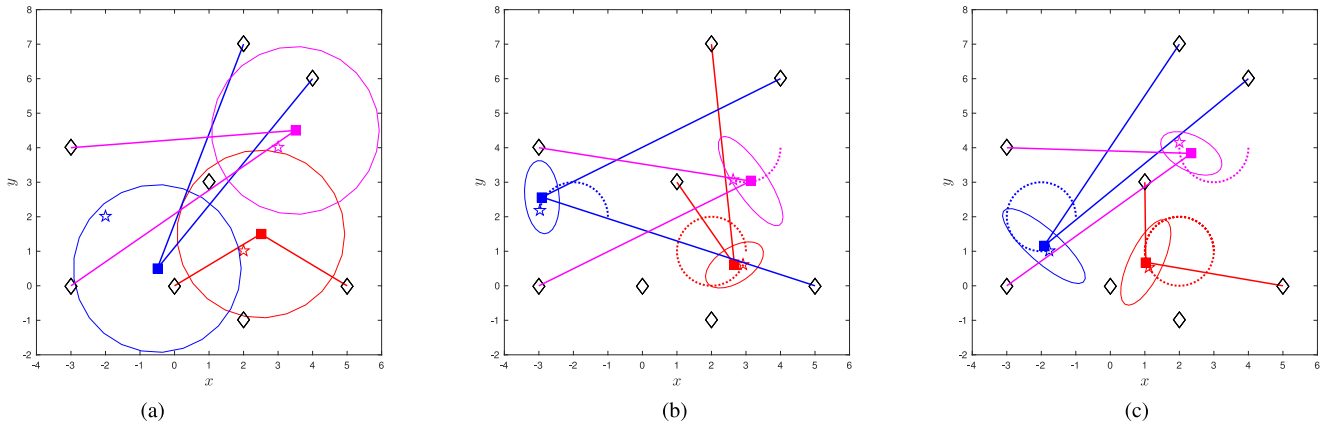


Fig. 4. Greedy nonoverlapping pair assignment (Algorithm 1) in action for tracking three targets with a circular motion by using  $\text{trace}(\mathbb{O}(p_{t_l}))$ . The three colors red, blue, and magenta specify three targets, respectively. The pentagram, filled square, solid ellipse (sometimes, it looks like a solid circle), and the dotted circle indicate the true position, estimate mean position, variance, and trajectory for the target, respectively. The black diamond indicates the sensor. The solid line joining the target and sensor indicates that the sensor is assigned to the target. (a)  $k = 1$  (initial time). (b)  $k = 60$ . (c)  $k = 100$ .

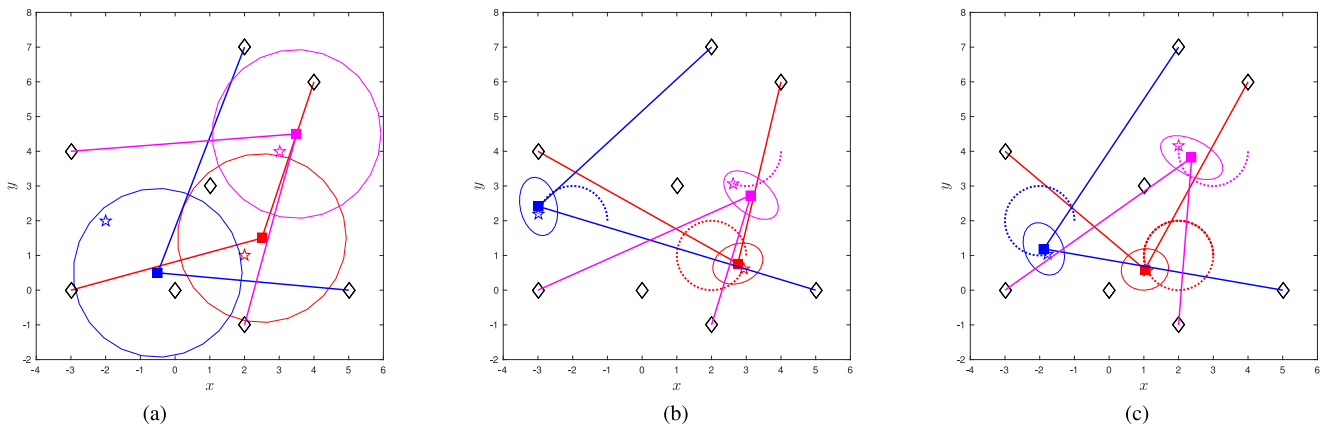


Fig. 5. Greedy nonoverlapping pair assignment (Algorithm 1) in action for tracking three targets with a circular motion by using  $\log \det(\mathbb{O}(p_{t_l}))$ . The three colors red, blue, and magenta specify three targets, respectively. The pentagram, filled square, solid ellipse (sometimes, it looks like a solid circle), and the dotted circle indicate the true position, estimate mean position, variance, and trajectory for the target, respectively. The black diamond indicates the sensor. The solid line joining the target and sensor indicates that the sensor is assigned to the target. (a)  $k = 1$  (initial time). (b)  $k = 60$ . (c)  $k = 100$ .

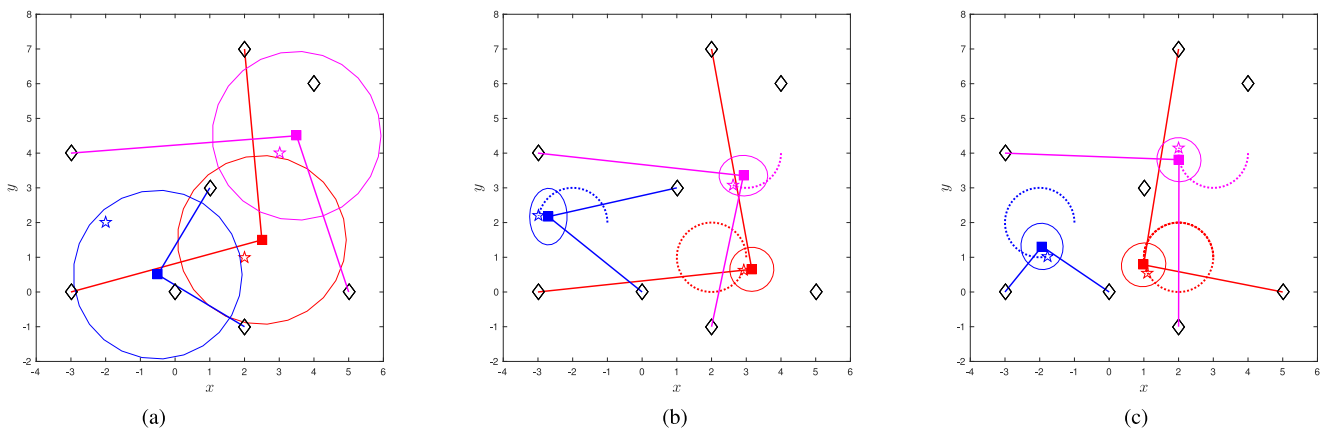
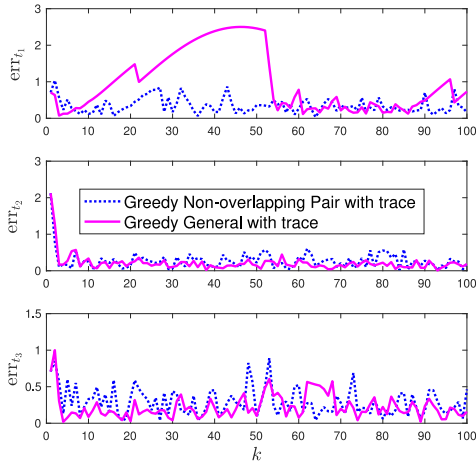
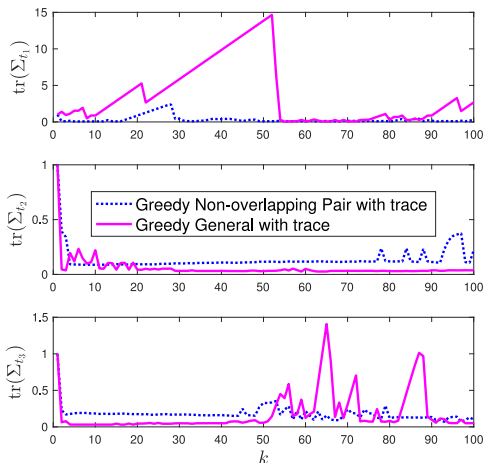


Fig. 6. Greedy nonoverlapping pair assignment (Algorithm 1) in action for tracking three targets with a circular motion by using  $\underline{C}^{-1}(\mathbb{O}(p_{t_l}, u_{t_l}))$ . The three colors red, blue, and magenta specify three targets, respectively. The pentagram, filled square, solid ellipse (sometimes, it looks like a solid circle), and the dotted circle indicate the true position, estimate mean position, variance, and trajectory for the target, respectively. The black diamond indicates the sensor. The solid line joining the target and sensor indicates that the sensor is assigned to the target. (a)  $k = 1$  (initial time). (b)  $k = 60$ . (c)  $k = 100$ .



(a)



(b)

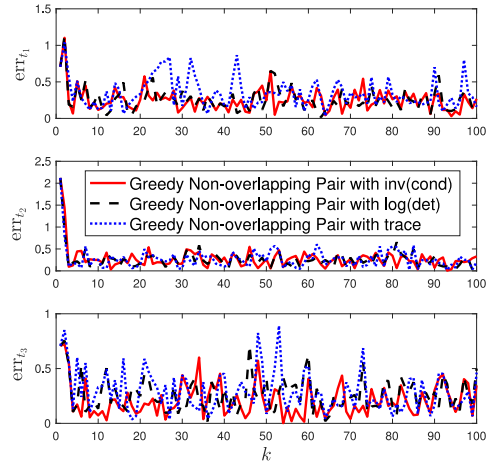
Fig. 7. Comparison of (a) mean error and (b) trace of covariance for three-target tracking within 100 time steps by greedy general assignment [26] with  $\text{trace}(\mathbb{O}(p_{t_l}))$  and greedy nonoverlapping pair assignment (Algorithm 1) with  $\text{trace}(\mathbb{O}(p_{t_l}))$ .

observability matrix,  $\underline{C}^{-1}(O(p_{t_l}, u_{t_l}))$ , for the assignment. The assignments for a specific scenario are shown in Figs. 5 and 6. Note that even though a pair of sensors is assigned to target  $t_l$ ,  $\mathbb{O}(p_{t_l})$  is not always nonsingular.

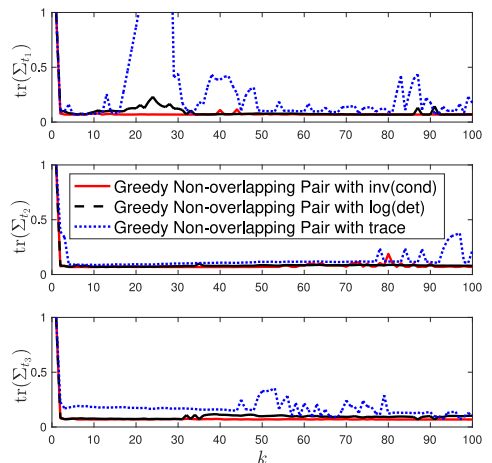
For each target  $t_l$ , the estimate generated by EKF includes its mean position  $\hat{p}_{t_l}$  and variance  $\Sigma_{t_l}$ ,  $l \in \{1, 2, 3\}$ . To evaluate the tracking performance, denote the mean error as

$$\text{err}_{t_l} = \|\hat{p}_{t_l} - p_{t_l}\|_2 \quad (11)$$

and the trace of covariance as  $\text{tr}(\Sigma_{t_l})$ . Fig. 7 shows  $\text{err}_{t_l}$  and  $\text{tr}(\Sigma_{t_l})$  for each target  $t_l$  with the greedy algorithms to the two assignment problem and with  $\text{trace}(\mathbb{O}(p_{t_l}))$  as the measure. We can observe that the greedy general assignment performs better for some target (e.g.,  $t_2$ ), but performs worse for target  $t_1$  as compared to the nonoverlapping pair assignment [see Fig. 7(b)]. Both algorithms maximize the sum of the observability measures for the three targets. In the nonoverlapping pair assignment, a pair of sensors is always assigned to each target, whereas in the



(a)



(b)

Fig. 8. Comparison of (a) mean error and (b) trace of covariance for three-target tracking within 100 time steps by greedy nonoverlapping pair assignment (Algorithm 1) with  $\underline{C}^{-1}(O(p_{t_l}))$ ,  $\log \det(\mathbb{O}(p_{t_l}))$ , and  $\text{trace}(\mathbb{O}(p_{t_l}))$ .

general assignment, there are situations where no sensors are assigned to a target. This can be due to the fact that it is profitable to assign more than two sensors to some target in order to maximize the sum. We can observe the happening in Fig. 2 where there exist some time steps (e.g.,  $k = 100$ ) when less than two sensors are assigned to a target (red), which leads to a bad tracking performance for individual targets in the general assignment case (see Corollary 1). However, in all cases, the greedy general assignment [26] ensures that the sum of individual measures is within a factor of 2 of the optimal sum.

Fig. 8 shows the tracking performance with the inverse condition number and log det is comparable. The performance with trace is worse as compared to the other two. However, we can only use the trace for the greedy general assignment, since it is submodular and monotone. This exactly reflects the importance of our greedy nonoverlapping pair assignment that better observability measures, i.e., log det and inverse condition number, which are not necessarily submodular and monotone, are also allowed.



### C. Baseline Comparisons

The nonoverlapping pair assignment (Problem 2) is NP-complete. Therefore, finding  $\omega(\text{OPT})$  is infeasible in polynomial time. In order to empirically evaluate the greedy nonoverlapping pair assignment (Algorithm 1), we use two baselines. When the number of sensors and targets is small, we compute the optimal solution using brute-force search. When the number of sensors and targets is large, we compute an upper bound on the optimal solution value by solving a relaxed version of Problem 2. In this relaxed version, one sensor is allowed to be assigned to multiple targets (unlike Problem 2). However, we still require a pair of sensors to be assigned to at most one specific target.

We formulate the new assignment as relaxed pair assignment (Problem 3). It is clear that solving relaxed pair assignment problem optimally gives us an upper bound of the optimality for nonoverlapping pair assignment problem. We can use this upper bound for the comparison of the greedy approach in nonoverlapping pair assignment.

**Problem 3 (Relaxed Pair Assignment):** Given a set of sensors,  $\mathcal{S} := \{s_0, \dots, s_N\}$ , and a set of targets,  $\mathcal{T} := \{t_0, \dots, t_L\}$ , find an assignment of nonrepetitive pairs of sensors to targets

$$\text{maximize } \sum_{l=1}^L \omega(\sigma_1(t_l), \sigma_2(t_l), t_l) \quad (12)$$

with the added constraint that all pairs are nonrepetitive, i.e.,  $\forall k, l = 1, \dots, L, k \neq l, \sigma_1(t_k) \neq \sigma_1(t_l)$  or  $\sigma_2(t_k) \neq \sigma_2(t_l)$ .

The relaxed pair assignment can be solved optimally by using maximum weight perfect bipartite matching (MWPBM) [35]. Note that a sensor can be matched in multiple distinct pairs and assigned to multiple targets. This violates the constraint in Problem 2 where each sensor can be matched to at most one pair and assigned at most once. The MWPBM can be solved using the Hungarian algorithm [14] in polynomial time.

While the relaxed pair assignment computes an upper bound for  $\omega(\text{OPT})$ , we can compute  $\omega(\text{OPT})$  exactly using the brute-force when  $N$  and  $L$  are small by enumerating all the possibilities. There are  $\prod_{l=0}^{L-1} \binom{N-2l}{2}$  possible cases. Thus, the brute-force algorithm has an exponential running time.

Fig. 9 shows the total value of the greedy algorithm,  $\omega(\text{GREEDY})$ , the brute-force algorithm,  $\omega(\text{OPT})$ , and the MWPBM,  $\omega(\text{MWPBM})$ , for log det and inverse condition number. We simulate the following environment:  $N = 2L$ , the positions of sensors and targets are generated randomly within  $[0, 100] \times [0, 100] \in \mathbb{R}^2$  for 30 trials for each  $L$ , and the target's maximum control input is  $u_{o,\max} = 1$ .

We run the comparison code on a MacBook Pro with 2.6 GHz Intel Core i5 and 8 GB memory. When  $L = 7$  and  $N = 14$ , MATLAB runs out of memory when running the brute-force algorithm (there are 681 080 400 possible cases for each trial). When  $L = 6$  and  $N = 12$ , the brute-force could not finish after running for 25 h. Thus, we only consider the case when  $L$  is varied from 1 to 5.

From Fig. 9, we observe that  $\omega(\text{MWPBM})$  is the highest because the MWPBM gives the upper bound of  $\omega(\text{OPT})$ . Specifically, the average of  $\omega(\text{GREEDY})/\omega(\text{OPT})$  and  $\omega(\text{GREEDY})/\omega(\text{MWPBM})$  for  $L = \{1, \dots, 5\}$  is as follows.

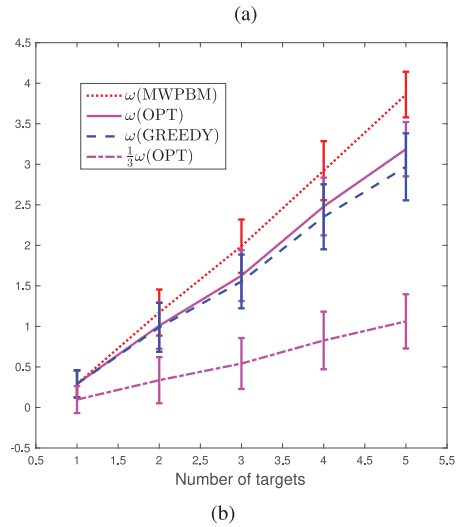
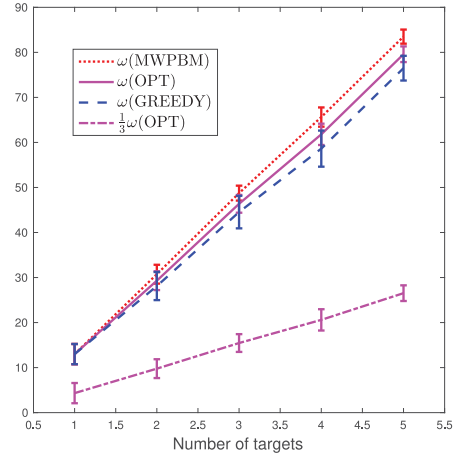


Fig. 9. Comparison of the total value charged by greedy approach (Algorithm 1) with the brute-force algorithm and the maximum perfect pair matching by using (a)  $\log \det \log(\det(\mathbb{O}(p_{t_l})))$  and (b) inverse condition number  $\underline{C}^{-1}(O(p_{t_l}, u_{t_l}))$ , respectively.

For the log det measure [see Fig. 9(a)],  $\omega(\text{GREEDY})/\omega(\text{OPT}) \approx 0.97$ , whereas  $\omega(\text{GREEDY})/\omega(\text{MWPBM}) \approx 0.93$ . For the inverse condition number [see Fig. 9(b)],  $\omega(\text{GREEDY})/\omega(\text{OPT}) \approx 0.96$ , whereas  $\omega(\text{GREEDY})/\omega(\text{MWPBM}) \approx 0.83$ . In both cases,  $\omega(\text{GREEDY})$  is close to  $\omega(\text{OPT})$  and much higher than the theoretical bound of  $\frac{1}{3}\omega(\text{OPT})$ , which suggests that in practice the algorithm works even better than the theoretical bound.

Next, we compare  $\omega(\text{GREEDY})$  and  $\omega(\text{MWPBM})$ , without the brute-force, for larger values of  $L$  and  $N$ . We vary  $L$  from 1 to 20 and set  $N = 2L$ . For both observability measures, Fig. 10 shows that  $\omega(\text{GREEDY})$  is close to  $\omega(\text{MWPBM})$  and much higher than  $\frac{1}{3}\omega(\text{MWPBM})$ . We also compute the average of  $\omega(\text{GREEDY})/\omega(\text{MWPBM})$  when  $L = \{1, \dots, 50\}$ . For the log det measure [see Fig. 10(a)],  $\omega(\text{GREEDY})/\omega(\text{MWPBM}) \approx 0.90$ . For the inverse condition number [see Fig. 10(b)],  $\omega(\text{GREEDY})/\omega(\text{MWPBM}) \approx 0.87$ . Thus, even though we give a theoretical 1/3-approximation for the greedy algorithm, it performs much better in practice. This is because the approximation ratio is obtained by considering the worst-case performance of the greedy algorithm.

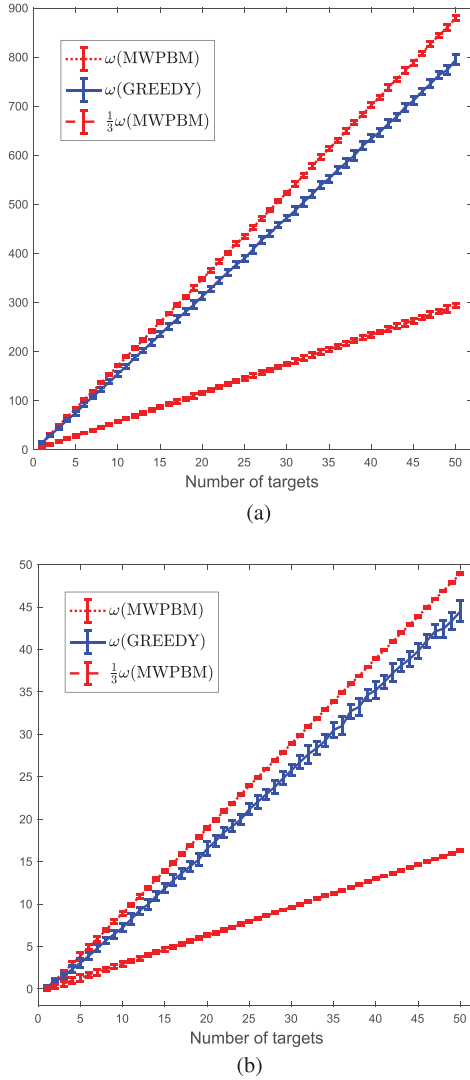


Fig. 10. Comparison of the total value charged by greedy approach (Algorithm 1) with the maximum perfect pair matching by using (a) log det  $\log(\det(\mathbb{O}(p_{t_i})))$  and (b) inverse condition number  $\underline{C}^{-1}(O(p_{t_i}, u_{t_i}))$ , respectively.

## VI. CONCLUSION

In this paper, we solved sensor assignment problems to improve the observability for target tracking. We derived the lower bound on the inverse of the condition number of the observability matrix for a system with a mobile target and  $N$  stationary sensors. The lower bound considers only the known part of the observability matrix—the sensor-target relative position and an upper bound on the target’s speed. We showed how this lower bound can be employed for sensor selection. We considered two sensor assignment problems for which we presented constant-factor approximation algorithms. While we presented the two algorithms as alternatives to each other, they can also be combined to give better results. We proved the log det,  $\log \det(\mathbb{O}(p_{t_i}))$ , is submodular and monotone only when  $\mathbb{O}(p_{t_i})$  is nonsingular and performs better in terms of tracking than the trace (which is submodular and monotone). We can combine the greedy general assignment with the greedy nonoverlapping pair assignment to use log det as the observability measure. First, we use the

nonoverlapping assignment to assign a pair of sensors to each target to make sure that  $\mathbb{O}(p_{t_i})$  is nonsingular. Then, we can improve the assignment strategy by using the greedy general assignment strategy to assign more sensors to each target.

Our immediate work is focused on assigning sensors to cover an area instead of tracking a group of targets. Another avenue is designing an efficient set covering strategy based on observability measures that are submodular and monotone. In many scenarios, the sensors are actually robots that are mobile [3], [36]–[42]. In such cases, in addition to solving the assignment problem, we can also optimize the trajectories of the sensors. An immediate future work is to devise joint assignment and planning algorithms for better observability.

Many of the results presented can be easily extended to 3-D tracking. We conjecture that at least three sensors will be required for ensuring nontrivial lower bounds of the inverse condition number in 3-D. The nonoverlapping pair assignment can be extended to assigning nonoverlapping triplets. We know that this algorithm will yield a  $1/4$ -approximation based on the general result given in Theorem 3.

## APPENDIX

### A. Proof for Theorem 1

*Proof:* The singular values of  $O(p_{t_i}, u_{t_i})$  can be found as the square root of the eigenvalues of the symmetric observability matrix,  $\mathbb{O}(p_{t_i}, u_{t_i})$ , given as [43]

$$\begin{aligned} \mathbb{O}(p_{t_i}, u_{t_i}) &= O^T(p_{t_i}, u_{t_i})O(p_{t_i}, u_{t_i}) \\ &= O^T(p_{t_i})O(p_{t_i}) + O^T(u_{t_i})O(u_{t_i}) \quad (13) \\ \begin{cases} \sqrt{\lambda_{\min}(\mathbb{O}(p_{t_i}, u_{t_i}))} = \sigma_{\min}(O(p_{t_i}, u_{t_i})) \\ \sqrt{\lambda_{\max}(\mathbb{O}(p_{t_i}, u_{t_i}))} = \sigma_{\max}(O(p_{t_i}, u_{t_i})) \end{cases} \quad (14) \end{aligned}$$

We can use *Weyl and dual Weyl* inequalities to bound the singular values. For Hermitian matrices  $X$  and  $Y$  with  $r$  eigenvalues written in increasing order  $\lambda_1(X) \leq \lambda_2(X) \leq \dots \leq \lambda_r(X)$  and  $\lambda_1(Y) \leq \lambda_2(Y) \leq \dots \leq \lambda_r(Y)$ , respectively, the *Weyl inequalities* [44] are given by

$$\lambda_{i+j-1}(X + Y) \geq \lambda_i(X) + \lambda_j(Y) \quad (15)$$

where  $i, j \geq 1$  and  $i + j - 1 \leq r$ . Similarly, the *dual Weyl inequalities* are given by

$$\lambda_{i+j-r}(X + Y) \leq \lambda_i(X) + \lambda_j(Y) \quad (16)$$

where  $i, j \geq 1$  and  $i + j - r \leq r$ .

Since  $\mathbb{O}(p_{t_i}, u_{t_i}) \in \mathbb{R}^{2 \times 2}$ ,  $O^T(p_{t_i})O(p_{t_i}) \in \mathbb{R}^{2 \times 2}$ , and  $O^T(u_{t_i})O(u_{t_i}) \in \mathbb{R}^{2 \times 2}$  are symmetric matrices, they are Hermitian with the eigenvalues (in ascending order) as  $\lambda_1(\mathbb{O}(p_{t_i}, u_{t_i})) \leq \lambda_2(\mathbb{O}(p_{t_i}, u_{t_i}))$ ,  $\lambda_1(O^T(p_{t_i})O(p_{t_i})) \leq \lambda_2(O^T(p_{t_i})O(p_{t_i}))$ , and  $\lambda_1(O^T(u_{t_i})O(u_{t_i})) \leq \lambda_2(O^T(u_{t_i})O(u_{t_i}))$ . Following the *Weyl and dual Weyl* inequalities, we get

$$\begin{aligned} \lambda_1(\mathbb{O}(p_{t_i}, u_{t_i})) &\geq \lambda_1(O^T(p_{t_i})O(p_{t_i})) + \lambda_1(O^T(u_{t_i})O(u_{t_i})) \\ \lambda_2(\mathbb{O}(p_{t_i}, u_{t_i})) &\leq \lambda_2(O^T(p_{t_i})O(p_{t_i})) + \lambda_2(O^T(u_{t_i})O(u_{t_i})). \quad (17) \end{aligned}$$

Thus

$$\begin{aligned} & \frac{\lambda_1(\mathbb{O}(p_{t_l}, u_{t_l}))}{\lambda_2(\mathbb{O}(p_{t_l}, u_{t_l}))} \\ & \geq \frac{\lambda_1(O^T(p_{t_l})O(p_{t_l})) + \lambda_1(O^T(u_{t_l})O(u_{t_l}))}{\lambda_2(O^T(p_{t_l})O(p_{t_l})) + \lambda_2(O^T(u_{t_l})O(u_{t_l}))}. \end{aligned} \quad (18)$$

Then, from (14) and (18), the inverse of the condition number of the local nonlinear observability matrix

$$\begin{aligned} C^{-1}(O(p_{t_l}, u_{t_l})) &= \sqrt{\frac{\lambda_1(\mathbb{O}(p_{t_l}, u_{t_l}))}{\lambda_2(\mathbb{O}(p_{t_l}, u_{t_l}))}} \\ &\geq \sqrt{\frac{\lambda_1(O^T(p_{t_l})O(p_{t_l})) + \lambda_1(O^T(u_{t_l})O(u_{t_l}))}{\lambda_2(O^T(p_{t_l})O(p_{t_l})) + \lambda_2(O^T(u_{t_l})O(u_{t_l}))}}. \end{aligned} \quad (19)$$

Thus, we have the lower of the inverse of the condition number

$$\sqrt{\frac{\lambda_1(O^T(p_{t_l})O(p_{t_l})) + \lambda_1(O^T(u_{t_l})O(u_{t_l}))}{\lambda_2(O^T(p_{t_l})O(p_{t_l})) + \lambda_2(O^T(u_{t_l})O(u_{t_l}))}}. \quad (20)$$

By calculating the eigenvalues of symmetric matrix of target's control contribution

$$O^T(u_{t_l})O(u_{t_l}) = \begin{bmatrix} u_{lx}^2 & u_{lx}u_{ly} \\ u_{lx}u_{ly} & u_{ly}^2 \end{bmatrix}$$

we have

$$\begin{aligned} \lambda_1(O^T(u_{t_l})O(u_{t_l})) &= 0 \\ \lambda_2(O^T(u_{t_l})O(u_{t_l})) &= u_{lx}^2 + u_{ly}^2 = u_{t_l}^2. \end{aligned} \quad (21)$$

Then, the lower bound of  $C^{-1}(O(o, u_o))$  [see (20)] is calculated as

$$\begin{aligned} \underline{C}^{-1}(O(p_{t_l}, u_{t_l})) &= \sqrt{\frac{\lambda_1(O^T(p_{t_l})O(p_{t_l}))}{\lambda_2(O^T(p_{t_l})O(p_{t_l})) + u_{t_l}^2}} \\ &= \frac{\sigma_{\min}(O(p_{t_l}))}{\sqrt{\sigma_{\max}^2(O(p_{t_l})) + u_{t_l}^2}}. \end{aligned} \quad (22)$$

Equation (22) gives the main lower bound. Note that  $C^{-1}(O(p_{t_l}, u_{t_l}))$  cannot be determined since target's control input  $u_{t_l}$  is unknown. However, we know that  $\|u_{t_l}\|_2 \leq u_{t_l, \max}$ . Therefore

$$\underline{C}^{-1}(O(p_{t_l}, u_{t_l})) \geq \frac{\sigma_{\min}(O(p_{t_l}))}{\sqrt{\sigma_{\max}^2(O(p_{t_l})) + u_{t_l, \max}^2}}. \quad (23)$$

This yields our main lower bound result.  $\blacksquare$

### B. Proof for Corollary 1

*Proof:* The local observability matrix for one-sensor-target  $s_i - t_l$  system can be derived from (5) as

$$O_i(p_{t_l}, u_{t_l}) = \begin{bmatrix} x_{t_l} - x_{s_i} & y_{t_l} - y_{s_i} \\ u_{lx} & u_{ly} \end{bmatrix}. \quad (24)$$

The sensor-target relative state contribution is

$$O_i(p_{t_l}) = [x_{t_l} - x_{s_i} \quad y_{t_l} - y_{s_i}]. \quad (25)$$

The  $s_i - t_l$  system is weakly locally observable if  $O_i(p_{t_l}, u_{t_l})$  has full column rank, i.e.,  $(x_{t_l} - x_{s_i})u_{ly} \neq (y_{t_l} - y_{s_i})u_{lx}$ . However, the sensor does not know the target's control input  $u_{t_l}$ .

Given the symmetric matrix by sensor-target relative state contribution of  $s_i - t_l$  system

$$O_i^T(p_{t_l})O_i(p_{t_l}) = \begin{bmatrix} (x_{t_l} - x_{s_i})^2, & (x_{t_l} - x_{s_i})(y_{t_l} - y_{s_i}) \\ (x_{t_l} - x_{s_i})(y_{t_l} - y_{s_i}), & (y_{t_l} - y_{s_i})^2 \end{bmatrix} \quad (26)$$

we have

$$\begin{cases} \sigma_{\min}(O_i(p_{t_l})) = \sqrt{\lambda_{\min}(O_i^T(p_{t_l})O_i(p_{t_l}))} = 0 \\ \sigma_{\max}(O_i(p_{t_l})) = \sqrt{\lambda_{\max}(O_i^T(p_{t_l})O_i(p_{t_l}))} \\ = \sqrt{(x_{t_l} - x_{s_i})^2 + (y_{t_l} - y_{s_i})^2} \end{cases}. \quad (27)$$

Thus, from (22), the lower bound for  $C^{-1}(O_i(p_{t_l}, u_{t_l}))$  is  $\frac{\sigma_{\min}(O_i(p_{t_l}))}{\sqrt{\sigma_{\max}^2(O_i(p_{t_l})) + u_{t_l}^2}} = 0$ . Consequently, the lower bound cannot be controlled by the sensor.  $\blacksquare$

### C. Proof for Corollary 2

*Proof:* According to (14), we have

$$\frac{\sigma_{\min}(O(p_{t_l}, u_{t_l}))}{\sigma_{\max}(O(p_{t_l}, u_{t_l}))} = \frac{\sqrt{\lambda_{\min}(\mathbb{O}(p_{t_l}, u_{t_l}))}}{\sqrt{\lambda_{\max}(\mathbb{O}(p_{t_l}, u_{t_l}))}}. \quad (28)$$

Following (18) and (21), we have the lower bound for  $\frac{\lambda_{\min}(\mathbb{O}(p_{t_l}, u_{t_l}))}{\lambda_{\max}(\mathbb{O}(p_{t_l}, u_{t_l}))}$ , described as

$$\frac{\lambda_{\min}(\mathbb{O}(p_{t_l}, u_{t_l}))}{\lambda_{\max}(\mathbb{O}(p_{t_l}, u_{t_l}))} \geq \frac{\lambda_{\min}(O^T(p_{t_l})O(p_{t_l}))}{\lambda_{\max}(O^T(p_{t_l})O(p_{t_l})) + u_{t_l}^2}. \quad (29)$$

Now, we equivalently rewrite the statement of the theorem (using eigenvalues instead of singular values) as: if

$$\begin{cases} \frac{\lambda_{\min}(O'^T(p_{t_l})O'(p_{t_l}))}{\lambda_{\max}(O'^T(p_{t_l})O'(p_{t_l}))} \geq \frac{\lambda_{\min}(O^T(p_{t_l})O(p_{t_l}))}{\lambda_{\max}(O^T(p_{t_l})O(p_{t_l}))} \\ \lambda_{\min}(O'^T(p_{t_l})O'(p_{t_l})) \geq \lambda_{\min}(O^T(p_{t_l})O(p_{t_l})) \end{cases} \quad (30)$$

then

$$\begin{aligned} & \frac{\lambda_{\min}(O'^T(p_{t_l})O'(p_{t_l}))}{\lambda_{\max}(O'^T(p_{t_l})O'(p_{t_l})) + u_{t_l}^2} \\ & \geq \frac{\lambda_{\min}(O^T(p_{t_l})O(p_{t_l}))}{\lambda_{\max}(O^T(p_{t_l})O(p_{t_l})) + u_{t_l}^2} \end{aligned} \quad (31)$$

where  $\lambda$  and  $\lambda'$  denote the eigenvalues before and after the sensors increase  $C^{-1}(O(p_{t_l}))$  and  $\sigma_{\min}(O(p_{t_l}))$ , respectively.

We start with the left-hand side of (31) to get

$$\begin{aligned} & \frac{\lambda'_{\min, l}}{\lambda'_{\max, l} + u_{t_l}^2} - \frac{\lambda_{\min, l}}{\lambda_{\max, l} + u_{t_l}^2} = \frac{\lambda'_{\min, l}\lambda_{\max, l} - \lambda'_{\max, l}\lambda_{\min, l}}{(\lambda'_{\max, l} + u_{t_l}^2)(\lambda_{\max, l} + u_{t_l}^2)} \\ & + \frac{u_{t_l}^2(\lambda'_{\min, l} - \lambda_{\min, l})}{(\lambda'_{\max, l} + u_{t_l}^2)(\lambda_{\max, l} + u_{t_l}^2)} \end{aligned} \quad (32)$$

where  $\lambda'_{\min, l}$ ,  $\lambda'_{\max, l}$ ,  $\lambda_{\min, l}$ , and  $\lambda_{\max, l}$  denote the simplified forms of  $\lambda_{\min}(O'^T(p_{t_l})O'(p_{t_l}))$ ,  $\lambda_{\max}(O'^T(p_{t_l})O'(p_{t_l}))$ ,

$\lambda_{\min}(O^T(p_{t_l})O(p_{t_l}))$ , and  $\lambda_{\max}(O^T(p_{t_l})O(p_{t_l}))$ , respectively. Note that (30) can be reordered to match the numerator in the second line of (32). Then, we have

$$\frac{\lambda'_{\min,l}}{\lambda'_{\max,l} + u_{t_l}^2} - \frac{\lambda_{\min,l}}{\lambda_{\max,l} + u_{t_l}^2} \geq 0. \quad (33)$$

■

*Remark 3:* Equation (30) is a sufficient, but not necessary condition to guarantee (31). This is because (31) can be established with a weaker condition

$$\lambda'_{\min,l}\lambda_{\max,l} - \lambda'_{\max,l}\lambda_{\min,l} + u_{t_l}^2(\lambda'_{\min,l} - \lambda_{\min,l}) \geq 0.$$

We choose the stricter condition [see (30)] because it is conceptually easy to separate and eliminate the influence on the degree of observability from target's control input  $u_{t_l}$ , which is unknown and uncontrolled.

#### D. Proof for Corollary 3

The proofs of the following lemmas follow the steps of the proofs in [34, Ths. 4, 6, and 7]. We first give the proofs of the properties of the *symmetric observability matrix by sensor-target relative state contribution*,  $\mathbb{O}(p_{t_l})$ . Then, we obtain the similar result for the *symmetric observability matrix*,  $\mathbb{O}(p_{t_l}, u_{t_l})$ , by a minor extension. For the target  $t_l$ , denote its sensor-target relative state vector as  $r_{il} = [x_{tl} - x_{si}, y_{tl} - y_{si}]$ ,  $i \in \{1, 2, \dots, N\}$ . Denote its ground sensor-target relative state set as  $\mathcal{V} = \{r_{1l}, r_{2l}, \dots, r_{Nl}\}$ . For a given  $\mathcal{W} \subseteq \mathcal{V}$ , we form  $R_{\mathcal{W}} = [R_{0l}, r_{wl}]^T$  with an (possibly empty) existing matrix  $R_{0l}$  and the associated sensor-target relative vector  $r_{wl} \in \mathcal{W}$ . We calculate the associated symmetric observability matrix by sensor-target relative state contribution as  $\mathbb{O}(p_{t_l})_{\mathcal{W}} = R_{wl}^T R_{wl}$ . To simplify notation, we write  $\mathbb{O}(p_{t_l})_{\mathcal{W}}$  as  $\mathbb{O}_{\mathcal{W}}$ .

*Lemma 1:* The set function mapping subsets  $\mathcal{W} \subseteq V$  to the trace of the associated symmetric observability matrix by sensor-target relative state contribution,  $f(\mathcal{W}) = \text{trace}(\mathbb{O}_{\mathcal{W}})$  is modular (submodular) and monotone increasing.

*Proof:* The symmetric observability matrix by sensor-target relative state contribution associated with  $\mathcal{W}$ ,  $\mathbb{O}_{\mathcal{W}}$  can be calculated as

$$\mathbb{O}_{\mathcal{W}} = R_{wl}^T R_{wl} = \sum_{r_{wl} \in \mathcal{W}} r_{wl}^T r_{wl}. \quad (34)$$

Thus, for any  $\mathcal{W} \subseteq V$ ,  $\mathbb{O}_{\mathcal{W}}$  is simply a sum of the symmetric observability matrix by sensor-target relative state contribution associated with the individual rows of  $R_{\mathcal{W}}$ . Given the trace is a linear matrix function, we have

$$\begin{aligned} f(\mathcal{W}) &= \text{trace}(\mathbb{O}_{\mathcal{W}}) \\ &= \text{trace} \sum_{r_{wl} \in \mathcal{W}} r_{wl}^T r_{wl} \\ &= \sum_{r_{wl} \in \mathcal{W}} \text{trace}(r_{wl}^T r_{wl}). \end{aligned} \quad (35)$$

If no sensors are assigned to the target  $t_l$ , define  $\text{trace}(\emptyset) = 0$ . Then, we have  $f(\mathcal{W}) = \text{trace}(\mathbb{O}_{\mathcal{W}})$  is a modular (submodular) and monotone increasing set function. ■

*Lemma 2:* The set function mapping subsets  $\mathcal{W} \subseteq V$  to the rank of the associated symmetric observability matrix by sensor-target relative state contribution,  $f(\mathcal{W}) = \text{rank}(\mathbb{O}_{\mathcal{W}})$  is submodular and monotone increasing.

*Proof:* Given two linear transformations  $Q_1, Q_2 \in \mathbb{R}^{n \times n}$ , we have

$$\begin{aligned} &\text{rank}(Q_1 + Q_2) \\ &= \text{rank}(Q_1) + \text{rank}(Q_2) \\ &\quad - \dim(\text{range}(Q_1) \cap \text{range}(Q_2)). \end{aligned} \quad (36)$$

From [45], we know that a set function  $f : 2^V \rightarrow \mathbb{R}$  is submodular if and only if the derived set functions  $f_r : 2^{V-\{r\}} \rightarrow \mathbb{R}$

$$f_r(\mathcal{W}) = f(\mathcal{W} \cup \{r\}) - f(\mathcal{W})$$

are monotone decreasing for all  $r \in \mathcal{V}$ . We can form the marginal gain functions for rank measure as

$$\begin{aligned} f_r(\mathcal{W}) &= \text{rank}(\mathbb{O}_{\mathcal{W} \cup r}) - \text{rank}(\mathbb{O}_{\mathcal{W}}) \\ &= \text{rank}(\mathbb{O}_r) - \dim(\text{range}(\mathbb{O}_{\mathcal{W}}) \cap \text{range}(\mathbb{O}_r)). \end{aligned} \quad (37)$$

Note that  $\text{rank}(\mathbb{O}_r)$  is a constant and  $\dim(\text{range}(\mathbb{O}_{\mathcal{W}}))$  only increases with  $\mathcal{W}$ . Thus,  $f_r$  is monotone decreasing, which means  $f(\mathcal{W}) = \text{rank}(\mathbb{O}_{\mathcal{W}})$  is a submodular function. From the additivity property of the  $\mathbb{O}_{\mathcal{W}}$  [see (34)], it is clear that  $f(\mathcal{W}) = \text{rank}(\mathbb{O}_{\mathcal{W}})$  is monotone increasing. ■

*Lemma 3:* The set function mapping subsets  $\mathcal{W} \subseteq V$  to the log det of the associated symmetric observability matrix by sensor-target relative state contribution,  $f(\mathcal{W}) = \log \det(\mathbb{O}_{\mathcal{W}})$  is submodular and monotone increasing if  $\mathbb{O}_{\mathcal{W}}$  is nonsingular.

*Proof:* We use the similar idea to show the submodularity of the log det measure, namely, showing that the derived set functions  $f_r : 2^{V-\{r\}} \rightarrow \mathbb{R}$

$$\begin{aligned} f_r(\mathcal{W}) &= \log \det(\mathbb{O}_{\mathcal{W} \cup r}) - \log \det(\mathbb{O}_{\mathcal{W}}) \\ &= \log \det(\mathbb{O}_{\mathcal{W}} + \mathbb{O}_r) - \log \det(\mathbb{O}_{\mathcal{W}}) \end{aligned}$$

are monotone decreasing for any  $r \in \mathcal{V}$ . Take any  $\mathcal{W}_1 \subseteq \mathcal{W}_2 \subseteq \mathcal{V} - \{r\}$ . By the additivity property of the  $\mathbb{O}_{\mathcal{W}}$  [see (34)], it is clear that  $\mathcal{W}_1 \subseteq \mathcal{W}_2 \Rightarrow \mathbb{O}_{\mathcal{W}_1} \preceq \mathbb{O}_{\mathcal{W}_2}$ . Define  $\mathbb{O}(\gamma) = \mathbb{O}_{\mathcal{W}_1} + \gamma(\mathbb{O}_{\mathcal{W}_2} - \mathbb{O}_{\mathcal{W}_1})$  for  $\gamma \in [0, 1]$ . Clearly,  $\mathbb{O}(0) = \mathbb{O}_{\mathcal{W}_1}$  and  $\mathbb{O}(1) = \mathbb{O}_{\mathcal{W}_2}$ . Now define

$$\hat{f}_r(\mathbb{O}(\gamma)) = \log \det(\mathbb{O}(\gamma) + \mathbb{O}_r) - \log \det(\mathbb{O}(\gamma)). \quad (38)$$

Note that  $\hat{f}_r(\mathbb{O}(0)) = \hat{f}_r(\mathbb{O}_{\mathcal{W}_1})$  and  $\hat{f}_r(\mathbb{O}(1)) = \hat{f}_r(\mathbb{O}_{\mathcal{W}_2})$ . We have

$$\begin{aligned} \frac{d}{d\gamma} \hat{f}_r(\mathbb{O}(\gamma)) &= \frac{d}{d\gamma} [\log \det(\mathbb{O}(\gamma) + \mathbb{O}_r) - \log \det(\mathbb{O}(\gamma))] \\ &= \text{trace}[(\mathbb{O}(\gamma) + \mathbb{O}_r)^{-1}(\mathbb{O}_{\mathcal{W}_2} - \mathbb{O}_{\mathcal{W}_1})] \\ &\quad - \text{trace}[(\mathbb{O}(\gamma))^{-1}(\mathbb{O}_{\mathcal{W}_2} - \mathbb{O}_{\mathcal{W}_1})] \\ &= \text{trace}[(\mathbb{O}(\gamma) + \mathbb{O}_r)^{-1} - (\mathbb{O}(\gamma))^{-1}](\mathbb{O}_{\mathcal{W}_2} - \mathbb{O}_{\mathcal{W}_1}) \\ &\leq 0. \end{aligned} \quad (39)$$

The second equality follows by the matrix derivative formula  $\frac{d}{dt} \log \det X(\gamma) = \text{trace}[X(\gamma)^{-1} \frac{d}{d\gamma} X(\gamma)]$  [46]. Notably, since  $\mathbb{O}(\gamma) \succeq 0$  and  $\mathbb{O}_r \succeq 0$ , we have  $\mathbb{O}(\gamma) + \mathbb{O}_r \succeq \mathbb{O}(\gamma)$  and thus  $(\mathbb{O}(\gamma) + \mathbb{O}_r)^{-1} - (\mathbb{O}(\gamma))^{-1} \preceq 0$ . Given  $(\mathbb{O}(\gamma) + \mathbb{O}_r)^{-1} - (\mathbb{O}(\gamma))^{-1} \preceq 0$ , and  $\mathbb{O}_{\mathcal{W}_2} - \mathbb{O}_{\mathcal{W}_1} \succeq 0$ , the last inequality holds. Since

$$\hat{f}_r(\mathbb{O}(1)) = \hat{f}_r(\mathbb{O}(0)) + \int_0^1 \frac{d}{d\gamma} \hat{f}_r(\mathbb{O}(\gamma)) d\gamma$$

it follows that  $\hat{f}_r(\mathbb{O}(1)) = \hat{f}_r(\mathbb{O}_{\mathcal{W}_2}) \leq \hat{f}_r(\mathbb{O}(0)) = \hat{f}_r(\mathbb{O}_{\mathcal{W}_1})$ . Thus, we have  $\hat{f}_r$  is monotone decreasing, and  $f$  is submodular. Similarly, the additivity property of  $\mathbb{O}_{\mathcal{W}}$  [see (34)] shows that  $f$  is monotone increasing.

However, the proof of the monotonicity and submodularity for the log det is based on the condition that  $\mathbb{O}(p_{t_i})$  is nonsingular. Otherwise, the conclusion does not hold. For example, if a single sensor is assigned to target  $t_i$ ,  $\mathbb{O}(p_{t_i})$  is always singular (see the proof of Corollary 1), and thus  $\log \det \mathbb{O}(p_{t_i}) = -\infty$ . If no sensors are assigned, we define the empty set case as  $\log \det(\emptyset) = 0$ . Then, the function is not monotone increasing.

The proof of the monotonicity and submodularity for the trace, rank, and log det of the *symmetric observability matrix*,  $\mathbb{O}(p_{t_i}, u_{t_i}) := O^T(p_{t_i}, u_{t_i})O(p_{t_i}, u_{t_i})$ , is similar to the proof for that of the *symmetric observability matrix by the sensor-target relative state contribution*,  $\mathbb{O}(p_{t_i})$ , as provided above. Because, from (13), we know

$$\mathbb{O}(p_{t_i}, u_{t_i}) = \mathbb{O}(p_{t_i}) + O^T(u_{t_i})O(u_{t_i}). \quad (40)$$

The *unknown control input contribution*  $O^T(u_{t_i})O(u_{t_i}) \succeq 0$  does not affect the properties of the measures for the *symmetric observability matrix*,  $\mathbb{O}(p_{t_i}, u_{t_i})$ , since assigning sensors only influences the *sensor-target relative state contribution part*,  $\mathbb{O}(p_{t_i})$ . But for the log det of *symmetric observability matrix*, we need to guarantee  $\mathbb{O}(p_{t_i}, u_{t_i})$  is nonsingular. ■

### E. Proof Sketch for Remark 2

First, by listing  $n + 1$  cases (similar to the three cases in the proof of Theorem 3), we show that there exists a many-to-one mapping  $\mathcal{M}_n : [1, \dots, L] \rightarrow [1, \dots, L]$  such that the following conditions hold:

- 1)  $\omega_n^*(k) \leq \omega_n^g(\mathcal{M}_n(k))$ ;
- 2)  $|\mathcal{M}_n^{-1}(y)| \leq n + 1$  for all  $y \in \mathcal{Y}$ , where  $\mathcal{Y} \subseteq [1, \dots, L]$  is the range of  $\mathcal{M}_n$ .

Denote  $\omega_n^*(k)$  and  $\omega_n^g(\mathcal{M}_n(k))$  as the values of the  $n + 1$ -tuple assigned to target  $t_k$  by OPT and to target  $\mathcal{M}_n(k)$  by GREEDY, respectively.

Second, following the steps in (10) and replacing the scalar 3 by  $n + 1$ , we reach the  $n + 1$  approximation in this general case.

### REFERENCES

- [1] B. Grocholsky, "Information-theoretic control of multiple sensor platforms," Ph.D. dissertation, Dept. Aerosp., Mechatronic Mech. Eng., Univ. Sydney, Sydney, NSW, Australia, 2002.
- [2] S. Jiang, R. Kumar, and H. E. Garcia, "Optimal sensor selection for discrete-event systems with partial observation," *IEEE Trans. Autom. Control*, vol. 48, no. 3, pp. 369–381, Mar. 2003.
- [3] J. R. Spletzer and C. J. Taylor, "Dynamic sensor planning and control for optimally tracking targets," *Int. J. Robot. Res.*, vol. 22, no. 1, pp. 7–20, 2003.
- [4] J. L. Williams, "Information theoretic sensor management," Ph.D. dissertation, Dept. Elect. Eng. Comput. Sci., Massachusetts Inst. Technol., Cambridge, MA, USA, 2007.
- [5] S. Kamath, E. Meisner, and V. Isler, "Triangulation based multi target tracking with mobile sensor networks," in *Proc. IEEE Int. Conf. Robot. Autom.*, 2007, pp. 3283–3288.
- [6] M. M. Zavlanos and G. J. Pappas, "Dynamic assignment in distributed motion planning with local coordination," *IEEE Trans. Robot.*, vol. 24, no. 1, pp. 232–242, Feb. 2008.
- [7] O. Tekdas and V. Isler, "Sensor placement for triangulation-based localization," *IEEE Trans. Autom. Sci. Eng.*, vol. 7, no. 3, pp. 681–685, Jul. 2010.
- [8] C. Nam and D. A. Shell, "When to do your own thing: Analysis of cost uncertainties in multi-robot task allocation at run-time," in *Proc. IEEE Int. Conf. Robot. Autom.*, 2015, pp. 1249–1254.
- [9] V. Tzoumas, A. Jadbabaie, and G. J. Pappas, "Sensor placement for optimal Kalman filtering: Fundamental limits, submodularity, and algorithms," in *Proc. Amer. Control Conf.*, 2016, pp. 191–196.
- [10] V. Tzoumas, A. Jadbabaie, and G. J. Pappas, "Near-optimal sensor scheduling for batch state estimation: Complexity, algorithms, and limits," in *Proc. IEEE 55th Conf. Decis. Control*, 2016, pp. 2695–2702.
- [11] V. Tzoumas, N. A. Atanasov, A. Jadbabaie, and G. J. Pappas, "Scheduling nonlinear sensors for stochastic process estimation," in *Proc. Amer. Control Conf.*, 2017, pp. 580–585.
- [12] F. Yang and N. Chakraborty, "Algorithm for optimal chance constrained linear assignment," in *Proc. IEEE Int. Conf. Robot. Autom.*, 2017, pp. 801–808.
- [13] S. Chopra, G. Notarstefano, M. Rice, and M. Egerstedt, "A distributed version of the Hungarian method for multirobot assignment," *IEEE Trans. Robot.*, vol. 33, no. 4, pp. 932–947, Aug. 2017.
- [14] H. W. Kuhn, "The Hungarian method for the assignment problem," *Nav. Res. Logist. Quart.*, vol. 2, no. 1/2, pp. 83–97, 1955.
- [15] A. S. Gadre and D. J. Stilwell, "Toward underwater navigation based on range measurements from a single location," in *Proc. IEEE Int. Conf. Robot. Autom.*, 2004, vol. 5, pp. 4472–4477.
- [16] G. Papadopoulos, M. F. Fallon, J. J. Leonard, and N. M. Patrikalakis, "Cooperative localization of marine vehicles using nonlinear state estimation," in *Proc. IEEE/RSJ Int. Conf. Intell. Robots Syst.*, 2010, pp. 4874–4879.
- [17] F. Arrichiello, G. Antonelli, A. P. Aguiar, and A. Pascoal, "An observability metric for underwater vehicle localization using range measurements," *Sensors*, vol. 13, no. 12, pp. 16191–16215, 2013.
- [18] R. K. Williams and G. S. Sukhatme, "Observability in topology-constrained multi-robot target tracking," in *Proc. IEEE Int. Conf. Robot. Autom.*, 2015, pp. 1795–1801.
- [19] P. Tokekar, J. Vander Hook, and V. Isler, "Active target localization for bearing based robotic telemetry," in *Proc. IEEE/RSJ Int. Conf. Intell. Robots Syst.*, 2011, pp. 488–493.
- [20] O. M. Cliff, R. Fitch, S. Sukkarieh, D. Saunders, and R. Heinsohn, "Online localization of radio-tagged wildlife with an autonomous aerial robot system," in *Proc. Robot., Sci. Syst.*, 2015, doi: [10.15607/RSS.2015.XI.042](https://doi.org/10.15607/RSS.2015.XI.042).
- [21] H. Bayram, K. Doddapaneni, N. Stefanos, and V. Isler, "Active localization of VHF collared animals with aerial robots," in *Proc. IEEE Int. Conf. Autom. Sci. Eng.*, 2016, pp. 934–939.
- [22] H. Van Nguyen, M. Chesser, L. P. Koh, S. H. Rezatofighi, and D. C. Ransinghe, "TrackerBots: Autonomous UAV for real-time localization and tracking of multiple radio-tagged animals," 2017, *arXiv:1712.01491*.
- [23] J. Thomas, J. Welde, G. Loianno, K. Daniilidis, and V. Kumar, "Autonomous flight for detection, localization, and tracking of moving targets with a small quadrotor," *IEEE Robot. Autom. Lett.*, vol. 2, no. 3, pp. 1762–1769, Jul. 2017.
- [24] M. Jafarizadeh and A. Zakerolhosseini, "Performance analysis of processing load distribution in camera networks for multi-target tracking," in *Proc. 9th Iranian Conf. Mach. Vis. Image Process.*, 2015, pp. 236–241.
- [25] E. Eriksson, G. Dán, and V. Fodor, "Distributed algorithms for feature extraction off-loading in multi-camera visual sensor networks," 2017, *arXiv:1705.08252*.
- [26] M. L. Fisher, G. L. Nemhauser, and L. A. Wolsey, "An analysis of approximations for maximizing submodular set functions—II," in *Polyhedral Combinatorics*. New York, NY, USA: Springer, 1978, pp. 73–87.
- [27] J. Vondrák, "Optimal approximation for the submodular welfare problem in the value oracle model," in *Proc. 40th Annu. ACM Symp. Theory Comput.*, 2008, pp. 67–74.
- [28] R. Hermann and A. Krener, "Nonlinear controllability and observability," *IEEE Trans. Autom. Control*, vol. AC-22, no. 5, pp. 728–740, Oct. 1977.

- [29] A. J. Krener and K. Ide, "Measures of unobservability," in *Proc. 48th IEEE Conf. Decis. Control/28th Chin. Control Conf.*, 2009, pp. 6401–6406.
- [30] F. J. Álvarez, T. Aguilera, J. A. Paredes, and J. A. Moreno, "Acoustic tag identification based on noncoherent FSK detection with portable devices," *IEEE Trans. Instrum. Meas.*, vol. 67, no. 2, pp. 270–278, Feb. 2018.
- [31] K. Hausman, J. Preiss, G. S. Sukhatme, and S. Weiss, "Observability-aware trajectory optimization for self-calibration with application to UAVs," *IEEE Robot. Autom. Lett.*, vol. 2, no. 3, pp. 1770–1777, Jul. 2017.
- [32] J. A. Preiss, K. Hausman, G. S. Sukhatme, and S. Weiss, "Simultaneous self-calibration and navigation using trajectory optimization," *Int. J. Robot. Res.*, vol. 37, no. 13/14, pp. 1573–1594, 2018.
- [33] J. Vander Hook, P. Tokekar, E. Branson, P. Bajer, P. Sorensen, and V. Isler, "Local-search strategy for active localization of multiple invasive fish," in *Experimental Robotics* (Springer Tracts in Advanced Robotics), vol. 88, J. P. Desai, G. Dudek, O. Khatib, and V. Kumar, Eds. New York, NY, USA: Springer, 2013, pp. 859–873.
- [34] T. H. Summers, F. L. Cortesi, and J. Lygeros, "On submodularity and controllability in complex dynamical networks," *IEEE Trans. Control Netw. Syst.*, vol. 3, no. 1, pp. 91–101, Mar. 2016.
- [35] T. H. Cormen, *Introduction to Algorithms*. Cambridge, MA, USA: MIT Press, 2009.
- [36] S. Martínez and F. Bullo, "Optimal sensor placement and motion coordination for target tracking," *Automatica*, vol. 42, no. 4, pp. 661–668, 2006.
- [37] G. Hollinger, S. Singh, J. Djughash, and A. Kehagias, "Efficient multi-robot search for a moving target," *Int. J. Robot. Res.*, vol. 28, no. 2, pp. 201–219, 2009.
- [38] T. H. Chung, J. W. Burdick, and R. M. Murray, "A decentralized motion coordination strategy for dynamic target tracking," in *Proc. IEEE Int. Conf. Robot. Autom.*, 2006, pp. 2416–2422.
- [39] G. Huang, K. Zhou, N. Trawny, and S. I. Roumeliotis, "A bank of maximum a posteriori (MAP) estimators for target tracking," *IEEE Trans. Robot.*, vol. 31, no. 1, pp. 85–103, Feb. 2015.
- [40] L. Zhou and P. Tokekar, "Active target tracking with self-triggered communications," in *Proc. IEEE Int. Conf. Robot. Autom.*, 2017, pp. 2117–2123.
- [41] L. Zhou and P. Tokekar, "Active target tracking with self-triggered communications in multi-robot teams," *IEEE Trans. Autom. Sci. Eng.*, to be published, doi: [10.1109/TASE.2018.2867189](https://doi.org/10.1109/TASE.2018.2867189).
- [42] R. Khodayi-mehr, Y. Kantaros, and M. M. Zavlanos, "Distributed state estimation using intermittently connected robot networks," *IEEE Trans. Robot.*, vol. 35, no. 3, pp. 709–724, Jun. 2019.
- [43] G. Strang, *Linear Algebra and Its Applications*. New York, NY, USA: Academic, 1976.
- [44] J. N. Franklin, *Matrix Theory*. Chelmsford, MA, USA: Courier Corporation, 2012.
- [45] L. Lovász, "Submodular functions and convexity," in *Mathematical Programming The State of the Art*. New York, NY, USA: Springer, 1983, pp. 235–257.
- [46] K. B. Petersen and M. S. Pedersen, *The Matrix Cookbook*, vol. 7. Kongens Lyngby, Denmark: Tech. Univ. Denmark, 2008, p. 510.



**Lifeng Zhou** (S'17) received the B.S. degree from the Huazhong University of Science and Technology, Wuhan, China, in 2013, and the M.Sc. degree from Shanghai Jiao Tong University, Shanghai, China, in 2016, both in automation. He is currently working toward the Ph.D. degree in electrical and computer engineering with Virginia Tech, Blacksburg, VA, USA.

His research interests include multirobot coordination, event-based control, sensor assignment, and risk-averse decision making.



**Pratap Tokekar** (M'10) received the B.Tech. degree in electronics and telecommunication from the College of Engineering Pune, Pune, India, in 2008, and the Ph.D. degree in computer science from the University of Minnesota, Minneapolis, MN, USA, in 2014.

He is currently an Assistant Professor with the Department of Electrical and Computer Engineering, Virginia Tech, Blacksburg, VA, USA. Previously, he was a Postdoctoral Researcher with the General Robotics, Automation, Sensing and Perception Laboratory, University of Pennsylvania, Philadelphia, PA,

USA. His research interests include algorithmic and field robotics, and cyber-physical systems, and their applications to precision agriculture and environmental monitoring.

Dr. Tokekar is a recipient of the NSF CISE Research Initiation Initiative Award.